IEEE Access
Multidisciplinary | Rapid Review | Open Access Journal

Received May 26, 2019, accepted June 10, 2019, date of publication June 20, 2019, date of current version July 3, 2019.

Digital Object Identifier 10.1109/ACCESS.2019.2924016

SC-Fano Decoding of Polar Codes

MIN-OH JEONG, (Student Member, IEEE), AND SONG-NAM HONG, (Member, IEEE)
Department of Electrical and Computer Engineering, Ajou University, Suwon 16499, South Korea

Corresponding author: Song-Nam Hong (snhong@ajou.ac.kr)

This work was supported by the Future Combat System Network Technology Research Center Program of Defense Acquisition Program Administration and Agency for Defense Development under Grant UD160070BD.

ABSTRACT For finite-length polar codes, the standard successive cancellation (SC) decoding has been improved, such as SC-List (SCL), SC-Stack (SCS), and SC-Flip (SCF) decodings. In this paper, we present an alternative improvement of SC decoding by incorporating the Fano sequential decoding into SC decoding. This is referred to as SC-Fano decoding. Specifically, it can address the major drawback of SC decoding by enabling moving-backward when the reliability of an on-going path is not good enough. The SCS and SC-Fano decodings can be viewed as the sequential decoding for polar codes. In addition, for cyclic-redundancy-check (CRC) concatenated polar codes, we enhance SC-Fano decoding by leveraging the bit-flipping idea of SCF decoding. The simulation results demonstrate that the proposed SC-Fano decoding can provide better performance-complexity tradeoff than the existing decoding methods.

INDEX TERMS Polar codes, successive-cancellation (SC) decoding, sequential decoding.

I. INTRODUCTION

Polar codes, proposed by Arikan in [1], achieve the symmetric capacity of the binary-input discrete memoryless channels (BI-DMCs) under a low-complexity successive-cancellation (SC) decoding. For practical finite lengths, however, polar codes with SC decoding yield poor performances compared with the state-of-the-art Turbo and LDPC codes. In [2], SC-List (SCL) decoding was proposed, which can achieve the optimal maximum-likelihood (ML) performance with sufficiently large list size. Despite its superior performance, SCL decoding still suffers from high computational complexity, memory requirement, and lower decoding throughput.

Recently in [3] and [4], SC-Stack (SCS) decoding was proposed whose computational complexity is very close to that of SC decoding in high signal-to-noise ratio (SNR) regimes. It was shown that SCS decoding can have much lower decoding complexity than SCL decoding, in order to achieve the frame-error-rate (FER) $<10^{-2}$. In [5] and [6], the authors developed an improved path-metric and an efficient stack decoding algorithm for polar codes. In spite of its computational advantage, SCS decoding requires larger space-complexity and its performance is poor when the stack-size is small [3], [4]. Another improvement of SC decoding was proposed in [7] with the aid of cyclic-redundancy-check (CRC) code, which is referred to as SC-Flip (SCF) decoding. In this method, SC decoding is first performed to generate an initial estimated codeword. If it passes the CRC check, the overall decoding is completed. Otherwise, the additional SC decoding proceeds by flipping a single information-bit corresponding to the lowest log-likelihood ratios (LLRs). This process is repeated until either a valid codeword is found (i.e., CRC passes) or a maximum number of iterations (i.e., T_{max}) is performed. Some improvements of SCF decoding were also proposed in [8]–[13].

Our contributions: We propose an alternative improvement of SC decoding by appropriately leveraging the Fano sequential decoding [14]. This is referred to as SC-Fano decoding. It is remarkable that SCS and SC-Fano decodings can be thought of as the sequential decoding of polar codes as similarly in convolutional codes [14]. In SC-Fano decoding, the basic procedures of SC decoding are performed by allowing to move backward on a code tree when the reliability of an on-going path is not sufficient. Specifically, at every (SC) decoding stage, it decides whether to move forward along a current path or move backward to find a more likelihood path in which the decision is made by comparing the proposed path metric with a dynamic threshold. The proposed path-metric can capture the reliabilities of partial paths with various lengths, which are required for the fair comparisons of such paths. We notice that a similar path-metric has been proposed in [15] for SCS decoding. In addition, we introduce an early termination technique for the proposed

The associate editor coordinating the review of this manuscript and approving it for publication was Chi-Tsun Cheng.

SC-Fano decoding, which can significantly reduce the decoding complexity by eliminating unnecessary backward moving. For CRC-concatenated polar codes, we develop the so-called SCF-Fano decoding by incorporating the bit-flipping ides of SCF decoding into the proposed SC-Fano decoding. Finally, simulation results demonstrate that the proposed decoding can provide better performance-complexity tradeoff than the existing methods.

This paper is organized as follows. In Section II, we briefly explain the polar codes and the standard SC decoding. Section III describes the proposed SC-Fano decoding. In Section IV, we provide some improvement techniques of SC-Fano decoding and simulation results. Section V concludes the paper.

II. PRELIMINARIES

We review the encoding and the standard SC decoding of polar codes in [1]. The polar codes are uniquely defined by the $(N, K, \mathcal{A})$ where $N = 2^n$ and K represent the code length and the number of information bits, respectively, and $\mathcal{A} \subseteq \{1, ..., N\}$ denotes the information set which contains the indices of K information bits. In [1], the generator matrix of a polar code is obtained by $\mathbf{G}_N = G_2^{\otimes n}$ where $G_2 = \left[\begin{smallmatrix} 1 & 0 \\ 1 & 1 \end{smallmatrix}\right]$ and $\otimes$ represent the 2-by-2 Arikan kernel and the Kronecker product, respectively, and B_N denotes the bit-reversal permutation matrix. Then, the polar encoding is performed as

$$\mathbf{x}_1^N = \mathbf{u}_1^N B_N G_N, \tag{1}$$

where $u_1^N = (u_1, ..., u_N)$ represents a message-vector containing both the information bits and zero frozen bits. In convention, the frozen bits are set by zero, i.e., $u_i = 0$ for $i \in \mathcal{A}^c$.

Next, we explain the standard SC decoding which produces the estimated information-bit $\hat{u}_i$ for $i = 1, 2, .., N$ in that order, from the observation $y_1^N = (y_1, y_2, ..., y_N)$. For each SC decoding stage i, it decodes the information-bit $\hat{u}_i$ as

$$\hat{u}_i = \begin{cases} 0, & \text{if } i \in \mathcal{A}^c \\ \text{sign}\left(\log\left(\dfrac{\Pr(u_i = 0|\hat{\mathbf{u}}_1^{i-1}, y_1^N)}{\Pr(u_i = 1|\hat{\mathbf{u}}_1^{i-1}, y_1^N)}\right)\right) & \text{if } i \in \mathcal{A} \end{cases} \tag{2}$$

where $\text{sign}(x) = 1$ if $x > 0$ and $\text{sign}(x) = 0$, otherwise. Here, $\Pr(u_i|\hat{\mathbf{u}}_1^{i-1}, y_1^N)$ (called branch-metric) is efficiently computed in a recursive way (see [1] for details) and will be used in the proposed decodings.

III. THE PROPOSED SC-FANO DECODING

We propose a low-complexity SC-Fano decoding for polar codes, by incorporating the Fano sequential decoding [14] into the standard SC decoding. Specifically, at every (SC) decoding stage, it determines whether to move forward along a current path or move backward to find a new path with higher reliability. Here, the decision is made by comparing the proposed path metric (to be defined in Section III-A) with a dynamic threshold. We remark that the proposed path-metric is tailored to polar codes, differently from the so-called Fano metric used in convolutional codes [14]. The SCS and SC-Fano decodings can be thought of as the sequential decoding for polar codes. In the following subsections, we will define the proposed path-metric and describe the detailed procedures of SC-Fano decoding.

A. THE PATH-METRIC

As in convolutional codes [14], the path-metric of SC-Fano decoding plays a crucial role in determining its complexity. Unless it is well defined, unnecessary backward moving will occur frequently, thus leading to a higher computation complexity. As in the Fano sequential decoding [14], the path metric of SC-Fano decoding should satisfy the following two requirements:

1) It should be able to capture the reliabilities of associated (partial) paths;
2) It should be properly normalized for the *fair* comparisons of the reliabilities of partial paths with various lengths.

To construct the proposed path-metric, we start with the path-metric used in SCL decoding [2] due to satisfying the first requirement. The corresponding SCL path-metric is defined as

$$\mathcal{P}_{SCL}(\hat{u}_1^i) = \mathcal{P}_{SCL}(\hat{u}_1^{i-1}) + \log\left(\Pr(\hat{u}_i|\hat{u}_1^{i-1}, y_1^N)\right), \quad \textit{for } i = 1, \ldots, N \tag{3}$$

with initial value $\mathcal{P}_{SCL}(\hat{u}_1^0) = 0$. As noticed before, the branch-metric $\Pr(u_i|\hat{\mathbf{u}}_1^{i-1}, y_1^N)$ is efficiently computed in a recursive way (see [1] for details). Unfortunately, it should not be able to meet the requirement 2) as it tends to decrease as a (decoded) path-length grows. In fact, the second requirement is not necessary for SCL decoding since the equal-length paths are only compared. The use of this metric itself can increase the decoding complexity since, as the decoding-stage proceeds, the resulting path-metric tends not to pass the dynamic threshold T, regardless of its actual reliability. Accordingly, the overall decoding process can be stuck (i.e., moving forward and backward repeatedly). We address this problem by normalizing path metrics properly as follows. Let $p_e^{(i)}$ be an error-probability of the polarized (or synthesized) channel i. Note that it can be efficiently computed via density evolution (see Remark 1 for details). Our motivation for the proposed normalization is that for any length-ℓ path $\hat{u}_1^\ell = (\hat{u}_1, \ldots, \hat{u}_\ell)$, the corresponding path-metric can be upper-bounded as

$$\mathcal{P}_{SCL}(\hat{u}_1^i) \le \sum_{j=1}^{i} \log(1 - p_e^{(j)}), \tag{4}$$

where this bound can be achieved with $\hat{u}_1^\ell = u_1^\ell$ (the corrected information bits). Equivalently, we obtain

$$\max_{\hat{u}_1^i \in \{0,1\}^i} \mathcal{P}_{SCL}(\hat{u}_1^i) \approx \sum_{j=1}^{i} \log(1 - p_e^{(j)}). \tag{5}$$

Form this, the proposed path-metric is defined as

$$\mathcal{P}_{SC-Fano}(\hat{u}_1^i) = \mathcal{P}_{SC-Fano}(\hat{u}_1^{i-1}) + \log\left(\frac{\Pr(\hat{u}_i|\hat{u}_1^{i-1}, y_1^N)}{1-p_e^{(i)}}\right), \quad for\ i = 1, \ldots, N \quad (6)$$

with initial value $\mathcal{P}_{SC-Fano}(\hat{u}_1^0) = 0$, which satisfies the requirement 2) as the maximum path-metric (corresponding to a correct path) would be 0 regardless of a path-length. Also, this metric can be rewritten as

$$\mathcal{P}_{SC-Fano}(\hat{u}_1^i) = \mathcal{P}_{SCL}(\hat{u}_1^i) - \sum_{j=1}^{i} \log(1-p_e^{(j)}), \quad (7)$$

where the second-term enables the fair comparisons for the reliabilities of (partial) paths with various lengths. We would like to point out that a similar path-metric has been proposed in [15] for SCS decoding.

Remark 1: Although it is too complicated to compute $p_e^{(j)}$ exactly, there are efficient methods to compute it approximately. In this paper, it is efficiently computed via the density evolution approach with a Gaussian approximation (DE-GA) [16]–[18]. To be specific, $p_e^{(j)}$ is estimated as

$$p_e^{(j)} = Q\left(\sqrt{\mu^{(j)}/2}\right), \quad 1 \le j \le N, \quad (8)$$

where $Q(\cdot)$ denotes a conventional Q-function. Here, $\mu^{(j)}$ is computed recursively as

$$\mu_N^{(2j-1)} = \phi^{-1}(1-(1-\phi(\mu_{N/2}^{(j)}))^2) \quad (9)$$

$$\mu_N^{(2j)} = 2\mu_{N/2}^{(j)}, \quad (10)$$

with initial value $\mu_1^{(1)} = \frac{2}{\sigma^2}$ where σ^2 will be specifically defined in Section V and $\phi(\cdot)$ is defined as (see [18] for details)

$$\phi = \begin{cases} \exp(-0.4527x^{0.86} + 0.0218), & \text{if } 0 < x \le 10 \\ \sqrt{\frac{\pi}{2}}(1-\frac{10}{7x})\exp(-\frac{x}{4}), & \text{if } x > 10. \end{cases} \quad (11)$$

■

B. SC-FANO DECODING

We will provide the detailed procedures of SC-Fano decoding where the proposed path-metric in (6) is assumed. Likewise the other improvements of SC decoding (such as SCL and SCS decodings), SC-Fano decoding is also performed based on the code tree as illustrated in Figs. 1 and 2. All those decodings can be viewed as efficient tree-search algorithms. Recall that SC decoding only moves forward (e.g., in the direction from the root node to leaf nodes) on the code tree such that at every decoding stage, the path with a higher branch-metric is chosen among two candidate paths (see Fig. 1). In contrast, the proposed SC-Fano decoding moves either forward or backward according to a current path-metric and a current dynamic threshold T (see Fig. 2).

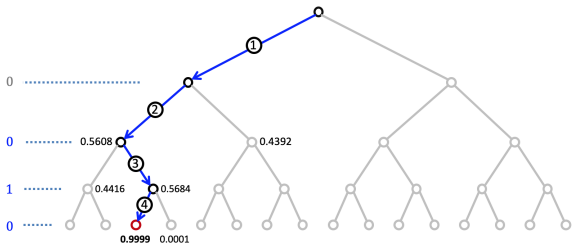

FIGURE 1. The example of SC decoding for the polar code with $N = 4$ and $R = \frac{3}{4}$. Here, it estimates the wrong message-vector $\hat{\mathbf{u}}_1^4 = (0, 0, 1, 0)$. The number beside the node denotes the branch-metric $\Pr(\hat{u}_i|\hat{\mathbf{u}}_1^{i-1}, \mathbf{y}_1^N)$.

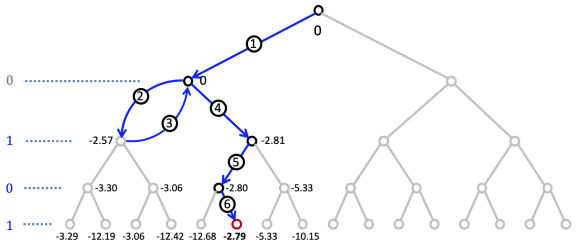

FIGURE 2. The example of SC-Fano decoding with $\Delta = 3$ for the polar code with $N = 4$ and $R = \frac{3}{4}$. Here, it estimates the correct message-vector $\hat{\mathbf{u}}_1^4 = (0, 1, 0, 1)$. The number beside node denotes the path-metric $\mathcal{P}_{SC-Fano}(\hat{\mathbf{u}}_1^i)$.

In SC-Fano decoding, each node can be reached with three different situations and the movement on the tree (e.g., forward or backward movement) is determined as follows. Let $\hat{u}_1^i = (\hat{u}_1, \ldots, \hat{u}_i)$ denote the decoded path up to now. For simplicity, we define

$$\alpha = \max_{\hat{u}_{i+1} \in \{0,1\}} \mathcal{P}_{SC-Fano}(\hat{u}_1^{i+1}). \quad (12)$$

Then, the detailed movement (or decoding) procedures at the current node $\hat{u}_i$ (not frozen node) are determined as follows:

a) The current node $\hat{u}_i$ is reached from the parent node $\hat{u}_{i-1}$ (as in SC decoding).
- $\alpha > T$: move forward along the current path as in SC decoding.
- $\alpha \le T$: move backward to the parent node $\hat{u}_{i-1}$ if $\mathcal{P}_{SC-Fano}(\hat{u}_1^{i-1}) > T$. Otherwise, the parent node and two child nodes have lower path metrics than the current threshold T. In this case, T decreases by the increment Δ and start decoding again at the current node $\hat{u}_i$.

b) The current node $\hat{u}_i$ is reached from the child node with a higher branch-metric.
- $\alpha > T$: move forward to the other child node with a lower branch-metric.
- $\alpha \le T$: move backward to the parent node $\hat{u}_1^{i-1}$ if $\mathcal{P}_{SC-Fano}(\hat{u}_1^{i-1}) > T$. Otherwise, as in the above, the current threshold T decreases by the increment Δ and start decoding again at the current node $\hat{u}_i$.

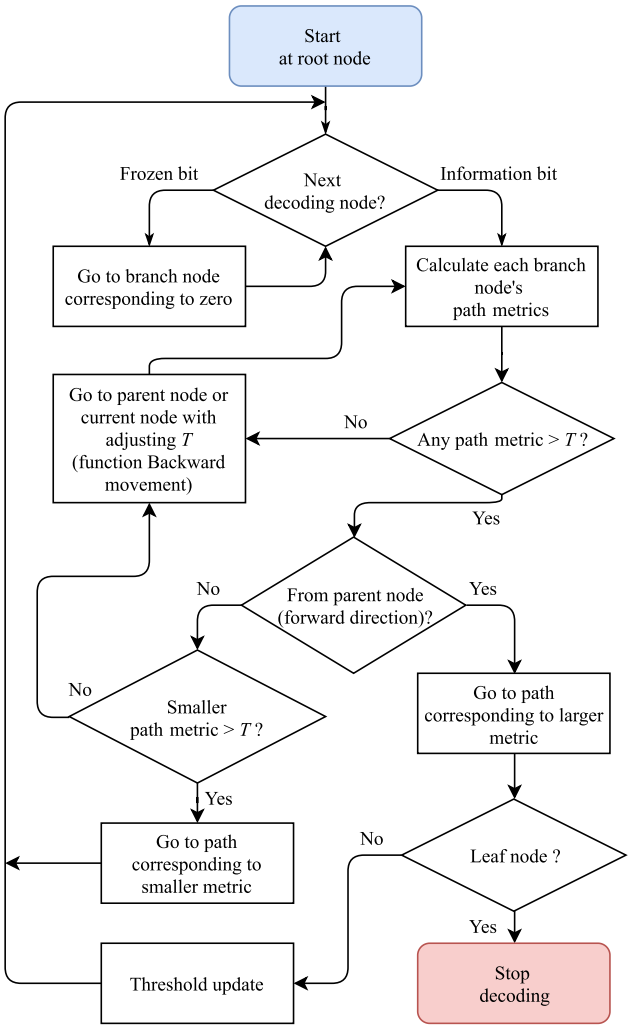

FIGURE 3. The flowchart of SC-Fano decoding.

c) The current node $\hat{u}_i$ is reached from the child node with a lower branch-metric.
   - move backward to the parent node $\hat{u}_1^{i-1}$ if $\mathcal{P}_{SC-Fano}(\hat{u}_1^{i-1}) > T$. Otherwise, as in the above, the current threshold T decreases by the increment Δ and start decoding again at the current node $\hat{u}_i$.

Note that in every frozen-bit decoding stage, SC-Fano decoding just moves forward to the zero-path, and also for the movement to a parent node (upper node), it skips the frozen nodes until reaching to the first information-bit node. SC-Fano decoding will stop when the decoded path-length is equal to N. The flow chart of SC-Fano decoding is provided in Fig. 3 and the corresponding detailed algorithms are provided in Algorithms 1, 2, and 3. Algorithm 1 describes the main structure of SC-Fano decoding. Here, a binary variable B indicates whether a current node is reached from a parent node (e.g., $B = 0$) or a child node (e.g., $B = 1$). $\boldsymbol{\gamma} = (\gamma_1, \ldots, \gamma_K)$ denotes the length-K binary vector where $\gamma_j = 1$ if the j-th information bit is decoded following the path with a lower branch-metric among the two candidate paths, and $\gamma_j = 0$, otherwise. To avoid recomputing the path metrics of revisited paths, the length-K vector $\boldsymbol{\beta} = (\beta_1, \ldots, \beta_K)$ is introduced where β_j contains the branch-metric for the j-th information bit. Algorithm 2 describes the procedures of the backward movements in SC-Fano decoding where it is activated only when both path metrics in a forward direction are lower than a current threshold T.

Algorithm 1 SC-Fano(y_1^N, Δ, $\mathcal{A}$)

Initialization: $i \leftarrow 1, j \leftarrow 0, B \leftarrow 0$
$\boldsymbol{\beta} = (\beta_1, \ldots, \beta_K) = 0, \boldsymbol{\gamma} = (\gamma_1, \ldots, \gamma_K) = 0$
while $i \neq N + 1$ **do**
  if $i \in \mathcal{A}$ **then** $m_{i,b} \triangleq \mathcal{P}(\hat{\mathbf{u}}_1^{i-1}, \hat{u}_i = b)$ for $b \in \{0, 1\}$
    if $\max\{m_{i,0}, m_{i,1}\} > T$ **then**
      if $B = 0$ **then** $\hat{u}_i = \text{argmax}\{m_{i,0}, m_{i,1}\}$,
        $\beta_{j+1} = \max\{m_{i,0}, m_{i,1}\}$, $\gamma_{j+1} = 0$
        if $j = 0$ **then** $\mu = 0$
        else if $j \neq 0$ **then** $\mu = \beta_j$
        end if
        if $\mu < T + \Delta$ **then** $T = \mathcal{U}(T, \Delta, \beta_{j+1})$
        end if
        $i = i + 1, j = j + 1$
      else if $B = 1$ **then**
        if $\min\{m_{i,0}, m_{i,1}\} > T$ **then**
          $\hat{u}_i = arg\ min\{m_{i,0}, m_{i,1}\}$,
          $\beta_{j+1} = \min\{m_{i,0}, m_{i,1}\}$, $\gamma_{j+1} = 1$
          $i = i + 1, j = j + 1, B = 0$
        else if $\min\{m_{i,0}, m_{i,1}\} \leq T$ **then**
          if $j = 0$ **then** $T = T - \Delta, B = 0$
          else if $j \neq 0$ **then**
            $(T, j, B) = \mathcal{B}(\boldsymbol{\beta}, j, T, \boldsymbol{\gamma})$,
            $i = \mathcal{A}(j + 1)$
          end if
        end if
      end if
    else if $\max\{m_{i,0}, m_{i,1}\} \leq T$ **then**
      if $j = 0$ **then** $T = T - \Delta$
      else if $j \neq 0$ **then**
        $(T, j, B) = \mathcal{B}(\boldsymbol{\beta}, j, T, \boldsymbol{\gamma}), i = \mathcal{A}(j + 1)$
      end if
    end if
  else if $i \notin \mathcal{A}$ **then** $\hat{u}_i = 0, i = i + 1$
  end if
end while
Return $\hat{\mathbf{u}}_1^N$

Remark 2: In SC-Fano decoding, a parameter Δ is used to control the performance-complexity tradeoff. For example, the performance of SC-Fano decoding can be enhanced by choosing a smaller value Δ while the corresponding computational complexity will increase as this tends to search more nodes on the code tree. Accordingly, when Δ is sufficiently small, it can achieve the performance of the optimal ML decoding. In contrast, if a larger value Δ is chosen, the performance of SC-Fano decoding will be degraded while reducing

the computational complexity. When Δ is sufficiently large, thus, SC-Fano decoding is equivalent to the standard SC decoding.

■

Algorithm 2 Backward Movement $\mathcal{B}(\boldsymbol{\beta}, j, T, \boldsymbol{\gamma})$

while True **do**
  if $j = 1$ **then** $\mu = 0$
  else if $j \geq 2$ **then** $\mu = \beta_{j-1}$
  end if
  if $\mu \geq T$ **then** $j = j - 1$
    if $\gamma_{j+1} = 0$ **then** $B = 1$, Return (T, j, B)
    end if
  else if $\mu < T$ **then** $T = T - \Delta$, $B = 0$
    Return (T, j, B)
  end if
end while

Algorithm 3 Threshold Update $\mathcal{U}(T, \Delta, \tau)$

while $T + \Delta < \tau$ **do** $T = T + \Delta$
end while
Return T

Example 1: In this example, we will show how the proposed SC-Fano decoding can outperform the standard SC decoding. For the comparison, we consider the polar code with the parameters $(N = 4, K = 3, \mathcal{A} = \{2, 3, 4\})$. Assuming the message-vector $u_1^4 = (0, 1, 0, 1)$, the polar encoding in (1) generates the codeword $x_1^4 = (0, 1, 0, 1)$. Considering the additive-white-Gaussian-noise (AWGN) channel and BPSK modulation, the (noisy) received signal is given as $y_1^4 = (1.4137, -1.5069, 2.3165, 1.3098)$. Figs. 1 and 2 illustrate the decoding procedures of SC and SC-Fano decodings, respectively. We used the parameter $\Delta = 3$ for SC-Fano decoding. This example shows that SC decoding fails to find a correct information-bit where $\hat{\mathbf{u}}_1^4 = (0, 0, 1, 0)$ is estimated. We notice that the failure of SC decoding is due to the wrong decision of $\hat{u}_2$ (e.g., ② in Fig. 1). In contrast, SC-Fano decoding can recognize this wrong decision as the path-metric is lower than the current threshold $T = -3$, namely, $\max\{\mathcal{P}(\hat{u}_1^2, \hat{u}_3 = 0), \mathcal{P}(\hat{u}_1^2, \hat{u}_3 = 1)\} = \max\{-3.30, -3.06\} = -3.06 < T = -3$. Here, note that the dynamic threshold was updated from $T = 0$ to $T = -3$ because both path metrics $\mathcal{P}(\hat{u}_1^2 = (0, 0)) = -2.57$ and $\mathcal{P}(\hat{u}_1^2 = (0, 1)) = -2.81$ in Fig. 2 are lower than $T = 0$. Algorithm 2 makes to move backward (e.g., ③ in Fig. 2). Also, from Algorithm 1, the decoding process moves along the other path (④ in the Fig. 2), which can eventually yield a correct information-bit $\hat{u}_1^4 = (0, 1, 0, 1)$. ■

IV. SOME DISCUSSIONS AND SIMULATION RESULTS

We present several techniques to improve the performance of the proposed SC-Fano decoding and then provide the simulation results to verify its good performance-complexity tradeoff.

A. IMPROVEMENTS OF SC-FANO DECODING

The proposed SC-Fano decoding is enhanced in two-fold. We first introduce an early termination technique which can reduce the computational complexity by removing unnecessary moving-backward operations. We then develop the so-called SCF-Fano decoding for CRC-concatenated polar codes, by combining SC-Fano decoding with the bit-flipping idea of SCF decoding.

1) EARLY TERMINATION

In SCF decoding, we keep tracking the dynamic threshold T which can capture the reliability of a current best path. The small value of T can imply that the current received value is too erroneous to be decoded correctly. Motivated by this, we can develop an early termination technique such that if the current threshold T is less than a pre-determined threshold T_e, SC-Fano decoding just performs the standard SC decoding in order to decode the rest of information bits. The complexity gains of this technique are provided in Fig. 10 and Fig. 11. From Figs. 10 and 11, we can see that T_e can control the performance-complexity tradeoff of SCF decoding. Thus, if we choose a proper threshold (e.g., $T_e = -25$ in Figs. 10 and 11), SC-Fano decoding can yield much better performance-complexity tradeoff.

Algorithm 4 SCF-Fano$(y_1^N, \mathcal{A}, T_{max})$

$(\hat{u}_1^N, L(y_1^N, \hat{u}_1^{i-1}|u_i)) \leftarrow$ SC-Fano$(\mathbf{Y}, \Delta, \mathcal{A}, v_1^N = \mathbf{0}, 0)$
$v_1^N = \hat{u}_1^N$ ▷ set the root path v_1^N
if $T_{max} > 1$ and CRC$(\hat{u}_1^N) =$ failure **then**
  $\mathcal{U} \leftarrow i \in \mathcal{A}$ of T_{max} smallest $|L(y_1^N, \hat{u}_1^{i-1}|u_i)|$
  for $j \leftarrow 1$ **to** T_{max} **do**
    $\mu \leftarrow \mathcal{U}(j)$
    $\hat{u}_1^N \leftarrow$ SC-Fano$(y_1^N, \Delta, \mathcal{A}, v_1^N, \mu)$
    if CRC$(\hat{u}_1^N) =$ success **then**
      Return $\hat{u}_1^N$
    end if
  end for
end if
Return $\hat{u}_1^N$

2) SCF-FANO DECODING

To further improve the performance, polar codes are frequently used together with CRC code. For this CRC-concatenated polar codes, we extend the proposed SC-Fano decoding by exploiting the bit-flipping idea of SCF decoding in [7]. SCF decoding iteratively performs the standard SC decoding by flipping one-bit until CRC passes or a maximum number of decoding trials T_{max} is met. In the first iteration, SC decoding (denoted by $\mathbf{SC}(\mathbf{Y}, \mathcal{A}, 0)$) yields the decoded information bits $\hat{u}_1^N$ and the corresponding LLR values $L(\mathbf{Y}, \hat{u}_1^{i-1}|u_i), i = 1, 2, \ldots, N$. Based on the LLR values, we construct an ordered set $\mathcal{U} = \{\ell_1, \ldots, \ell_{T_{max}}\}$ containing the indices of T_{max} least reliable decoded bits. Then, the second SC decoding is performed by flipping the

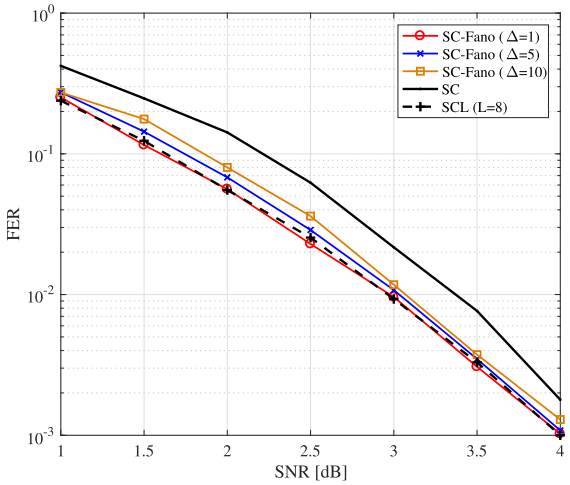

FIGURE 4. Performance comparisons of SC, SCL, and SC-Fano decodings for the length-128 polar code of the rate $\frac{1}{2}$.

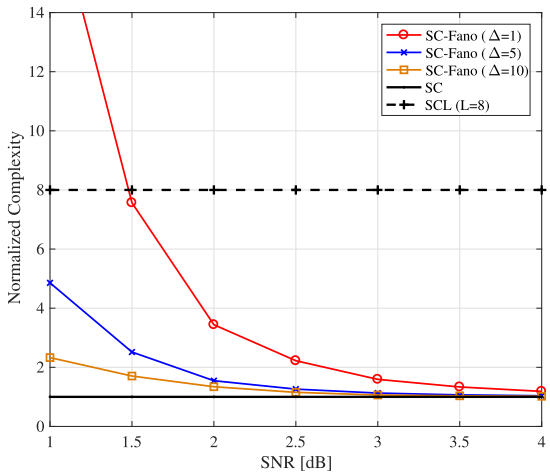

FIGURE 5. Complexity comparisons of SC, SCL, and SC-Fano decodings for the length-128 polar code of the rate $\frac{1}{2}$.

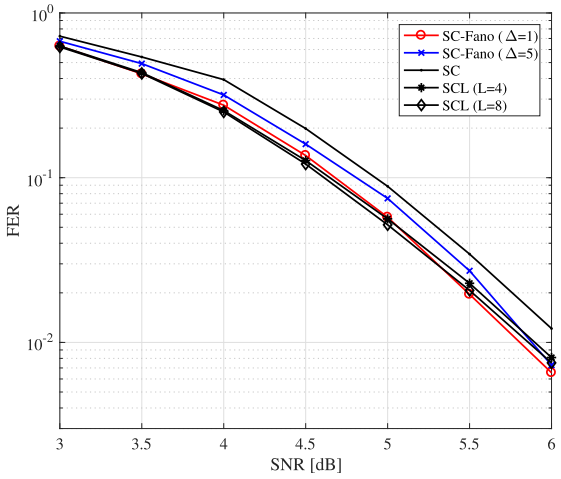

FIGURE 6. Performance comparisons of SC, SCL, and SC-Fano decodings for the length-128 polar code of the rate $\frac{3}{4}$.

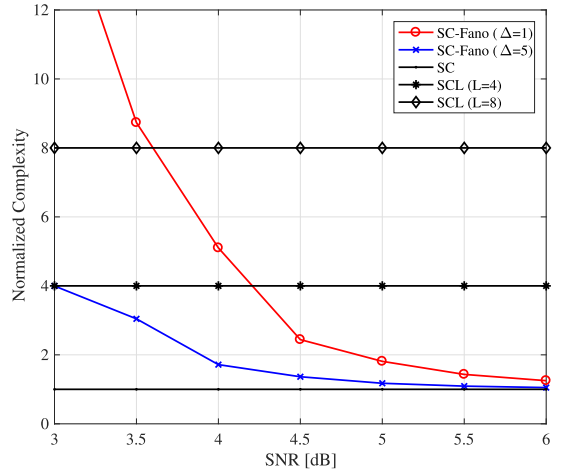

FIGURE 7. Complexity comparisons of SC, SCL, and SC-Fano decodings for the length-128 polar code of the rate $\frac{3}{4}$.

decoded bit indexed by ℓ_1. This process is repeated until decoding successes or the maximum number of trials is performed. Likewise, the proposed SCF-Fano decoding follows the above process with SC-Fano decoding instead of the standard SC decoding. The detailed procedures of SCF-Fano decoding are provided in Algorithm 4.

Remark 3: In the proposed SCF-Fano decoding, both Fano and CRC decodings can eliminate unnecessary paths in the tree search via soft-thresholding and hard-thresholding, respectively. Although SC-Fano decoding itself can achieve the optimal ML performance of a polar code with a proper parameter Δ, SCF-Fano decoding can outperform SC-Fano decoding by showing better BLER slope as in the CRC-concatenated SCL decoding [2]. ■

B. SIMULATION RESULTS

We provide the simulation results to verify an elegant performance-complexity tradeoff of the proposed SC-Fano and SCF-Fano decodings. For the simulations, we consider the frame-error-rate (FER) and the relative decoding complexity as the performance and complexity measures, respectively. Note the relative decoding complexity is computed by normalizing the complexities of decoding methods by the standard SC decoding, namely, the relative complexity of SC decoding is set by 1 (see Remark 4 below).

Remark 4: As the complexity measures, we employ the notion of *normalized* complexity where the complexities of SC, (Adaptive) SCL, (standard, Dynamic and Thresholded) SCF, SC-Fano, SCF-Fano decodings are normalized by the complexity of SC decoding. They are formally defined as

$$\chi_{SC-Fano} = \mathbb{E}[N_{SC-Fano}/N_{SC}], \quad (13)$$

$$\chi_{SCF-Fano} = \mathbb{E}[N_{SCF-Fano}/N_{SC}], \quad (14)$$

$$\chi_{SCL} = \mathbb{E}[N_{SCL}/N_{SC}], \quad (15)$$

$$\chi_{SCF} = \mathbb{E}[N_{SCF}/N_{SC}] \quad (16)$$

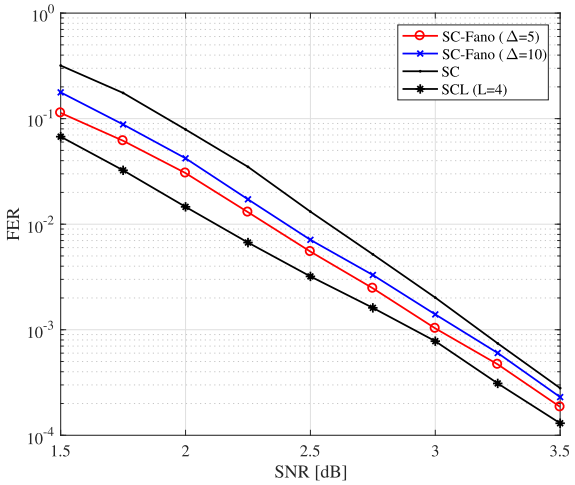

FIGURE 8. Performance comparisons of SC, SCL, and SC-Fano decodings for the length-1024 polar code of the rate $\frac{1}{2}$.

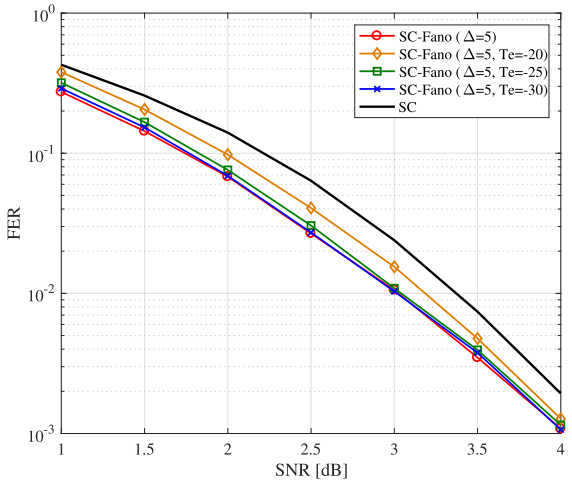

FIGURE 10. Performance comparisons of SC-Fano decoding for the length-128 polar code of the rate $R = \frac{1}{2}$ with various complexity reduction techniques.

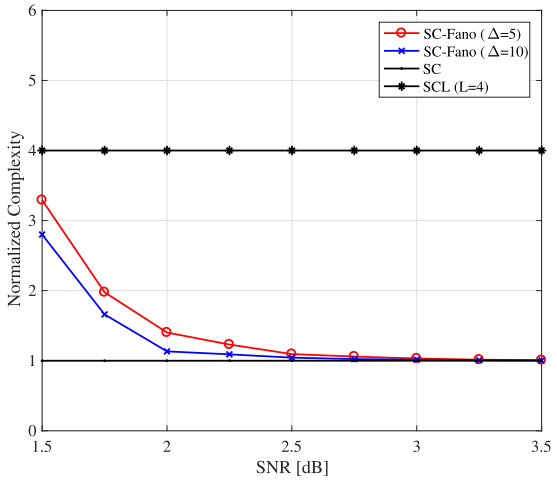

FIGURE 9. Complexity comparisons of SC, SCL, and SC-Fano decodings for the length-1024 polar code of the rate $\frac{1}{2}$.

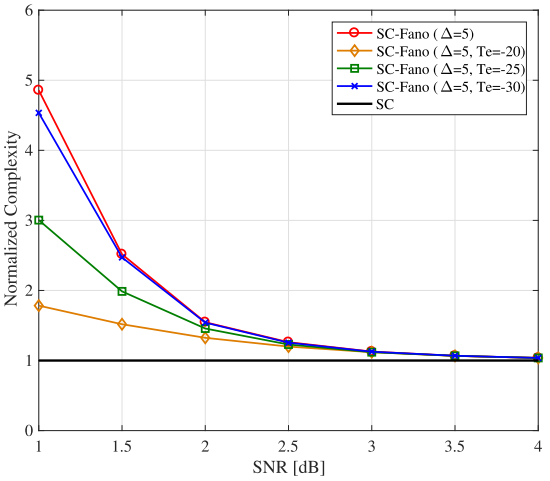

FIGURE 11. Complexity comparisons of SC-Fano decoding for the length-128 polar code of the rate $R = \frac{1}{2}$ with various complexity reduction techniques.

where N_{SC}, $N_{SC-Fano}$, $N_{SCF-Fano}$, N_{SCL}, and N_{SCF} denotes the summation of all the number of decoded bits during SC, SC-Fano, SCF-Fano, (Adaptive) SCL, and (Standard, Dynamic and Thresholded) SCF decodings, respectively. Clearly, N_{SC} is equal to the number of decoded bits (e.g., code length N). Although they are not an accurate comparisons of the decoding complexities, we believe that they can be used to measure the relative complexities over the standard SC decoding. ■

In the proposed decodings, $p_e^{(j)}$ (which is used to normalize the proposed path-metric) is efficiently computed via DE-GA in Remark 1 with the parameter $\sigma^2 = 10^{-0.1}$ and $\sigma^2 = 10^{-0.3}$ (e.g., SNR $= 1$ and SNR $= 3$ dB) for the code rates $1/2$ and $3/4$, respectively. AWGN channel and the polar code of length-128 and rate $1/2$ are assumed in which an information set is obtained using a predetermined ordering sequence proposed in [19]. For SCL decoding, the list-size $L = 4$ and 8 are used.

Figs. 4 and 5 show the FER and complexity comparisons of various decoding methods for the polar code of rate $1/2$ where CRC is not used. We can confirms that the parameter Δ plays an important role in controlling the performance-complexity tradeoff of the proposed SC-Fano decoding. Also, it is shown that SC-Fano decoding with $\Delta = 1$ can achieve the performance of SCL decoding with lower computational complexity. Here, the complexity reduction becomes larger as SNR increases. For the example of FER $= 10^{-2}$, SC-Fano decoding achieves the same performance with SCL decoding with the 25% computational complexity.

In Figs. 6 and 7, we performed the same comparisons with the higher-rate polar code (e.g., rate $3/4$). As seen before, SC-Fano decoding can also achieve the same performance of SCL decoding with reduced computational complexity. In addition, we have performance the comparisons for the longer-length polar code, which is provided in Figs. 8 and 9.

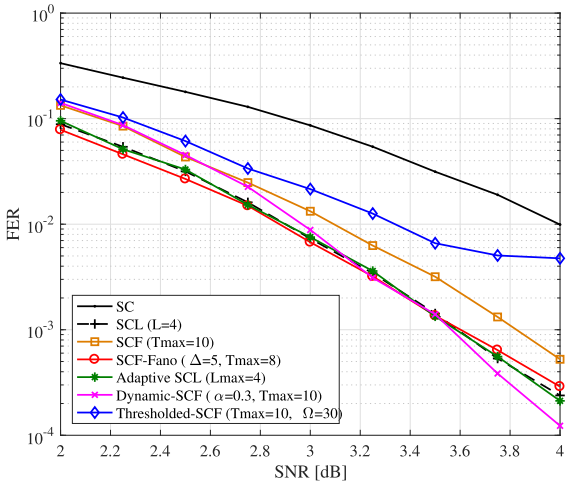

FIGURE 12. Performance comparisons of SC, SCL, Adaptive SCL, standard SCF, Dynamic-SCF, Thresholded-SCF, and SCF-Fano decoding for the length-128 polar code of the rate $R = \frac{1}{2}$ with 8-bit CRC.

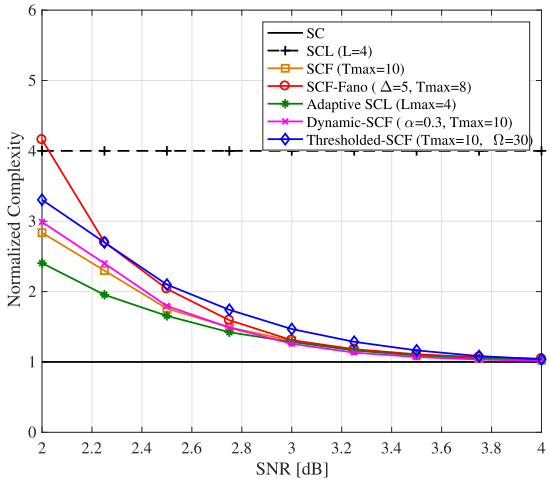

FIGURE 13. Complexity comparisons of standard SC, SCL, Adaptive SCL, standard SCF, Dynamic-SCF, Thresholded-SCF, and SCF-Fano decoding for the length-128 polar code of the rate $R = \frac{1}{2}$ with 8-bit CRC.

Compared to the short-length polar code, the performance gap between SCL ($L = 4$) and SC-Fano ($\Delta = 5$) decodings grows. However, we remark that, for a given normalized complexity gain, the actual complexity-reduction gain becomes larger as code length increases. Thus, the actual performance gap would be similar regardless of code lengths. Figs. 10 and 11 show that the proposed early termination technique can considerably reduce the complexity of SC-Fano decoding especially at lower SNR regimes.

In Figs. 12 and 13, we consider the CRC-concatenated polar codes and show the performance-complexity tradeoff of various decoding methods as SC, (standard) SCF, SCF-Fano, Dynamic-SCF [9], Thresholded-SCF [12], and Adaptive SCL [20] decodings. Here, we used 8-CRC with the generator polynomial $x^8 + x^7 + x^6 + x^4 + x^2 + 1$. Also, we selected $T_{max} = 10$ for standard SCF, Dynamic-SCF and Thresholded-SCF decodings, and $T_{max} = 8$ for SCF-Fano decoding. For Thresholded-SCF [12], we used a fixed critical set as {28, 77, 40, 57, 83, 30, 98, 85, 31, 44} for $T_{max} = 10$, which is calculated at 3dB SNR, and used the threshold as $\Omega = 30$. We observe that the proposed SCF-Fano decoding can achieve the performance of SCL decoding with a lower computational complexity as well as significantly outperforms SC decoding with an almost same complexity. Also, SCF-Fano decoding can achieve the almost same performance-complexity tradeoff at interesting moderate to high SNR regimes. It is remarkable that Adaptive SCL decoding requires a large size hardware implementation according to its maximum list-size decoding, while SCF-Fano decoding does not. Therefore, we can say that the proposed SCF-Fano decoding yields better performance-complexity tradeoff than the existing decodings.

V. CONCLUSION

We proposed the improvement of the standard SC decoding, named SC-Fano decoding, by incorporating the Fano sequential decoding into SC decoding. Also, we further reduced its decoding complexity by introducing an early-termination technique by leveraging a dynamic threshold which is naturally obtained during SC-Fano decoding. For CRC-concatenated polar codes, we extended SC-Fano decoding using the bit-flipping idea of SCF decoding. Simulation results demonstrated that the proposed SCF decodings yield better performance-complexity tradeoff than the existing various decoding methods as SCS, SCL, and SCF decodings. An interesting future work is to study the theoretical analysis on the decoding complexity of SC-Fano decoding as a function of SNRs.

REFERENCES

[1] E. Arikan, "Channel polarization: A method for constructing capacity-achieving codes for symmetric binary-input memoryless channels," *IEEE Trans. Inf. Theory*, vol. 55, no. 7, pp. 3051–3073, Jul. 2009.

[2] I. Tal and A. Vardy, "List decoding of polar codes," *IEEE Trans. Inf. Theory*, vol. 61, no. 5, pp. 2213–2226, May 2015.

[3] K. Niu and K. Chen, "Stack decoding of polar codes," *Electron. Lett.*, vol. 48, no. 12, pp. 695–697, Jun. 2012.

[4] K. Chen, K. Niu, and J. Lin, "Improved successive cancellation decoding of polar codes," *IEEE Trans. Commun.*, vol. 61, no. 8, pp. 3100–3107, Aug. 2013.

[5] V. Miloslavskaya and P. Trifonov, "Sequential decoding of polar codes," *IEEE Commun. Lett.*, vol. 18, no. 7, pp. 1127–1130, Jul. 2014.

[6] P. Trifonov, "A score function for sequential decoding of polar codes," in *Proc. IEEE Int. Symp. Inf. Theory (ISIT)*, Vail, CO, USA, Jun. 2018, pp. 1470–1474.

[7] O. Afisiadis, A. Balatsoukas-Stimming, and A. Burg, "A low-complexity improved successive cancellation decoder for polar codes," in *Proc. 48th Asilomar Conf. Signals, Syst. Comput.*, Pacific Grove, CA, USA, Nov. 2014, pp. 2116–2120.

[8] L. Chandesris, V. Savin, and D. Declercq, "An improved SCFlip decoder for polar codes," in *Proc. IEEE Global Commun. Conf. (GLOBECOM)*, Washington, DC, USA, Dec. 2016, pp. 1–6.

[9] L. Chandesris, V. Savin, and D. Declercq, "Dynamic-SCFlip decoding of polar codes," *IEEE Trans. Commun.*, vol. 66, no. 6, pp. 2333–2345, Jun. 2018.

[10] C. Condo, F. Ercan, and W. J. Gross, "Improved successive cancellation flip decoding of polar codes based on error distribution," in *Proc. IEEE Wireless Commun. Netw. Conf. Workshops (WCNCW)*, Barcelona, Spain, Apr. 2018, pp. 19–24.

[11] F. Ercan, C. Condo, S. A. Hashemi, and W. J. Gross, "Partitioned successive-cancellation flip decoding of polar codes," in *Proc. IEEE Int. Conf. Commun. (ICC)*, May 2018, pp. 1–6.
[12] F. Ercan, C. Condo, and W. J. Gross, "Improved bit-flipping algorithm for successive cancellation decoding of polar codes," *IEEE Trans. Commun.*, vol. 67, no. 1, pp. 61–72, Jan. 2019.
[13] Z. Zhang, K. Qin, L. Zhang, H. Zhang, and G. T. Chen, "Progressive bit-flipping decoding of polar codes over layered critical sets," in *Proc. IEEE Global Commun. Conf. (GLOBECOM)*, Singapore, Dec. 2017, pp. 1–6.
[14] R. Fano, "A heuristic discussion of probabilistic decoding," *IEEE Trans. Inf. Theory*, vol. 9, no. 4, pp. 64–74, Apr. 1963.
[15] P. Trifonov and V. Miloslavskaya, "Polar codes with dynamic frozen symbols and their decoding by directed search," in *Proc. IEEE Inf. Theory Workshop (ITW)*, Sevilla, Spain, Sep. 2013, pp. 1–5.
[16] R. Mori and T. Tanaka, "Performance of polar codes with the construction using density evolution," *IEEE Commun. Lett.*, vol. 13, no. 7, pp. 519–521, Jul. 2009.
[17] P. Trifonov, "Efficient design and decoding of polar codes," *IEEE Trans. Commun.*, vol. 60, no. 11, pp. 3221–3227, Nov. 2012.
[18] S.-Y. Chung, T. J. Richardson, and R. L. Urbanke, "Analysis of sum-product decoding of low-density parity-check codes using a Gaussian approximation," *IEEE Trans. Inf. Theory*, vol. 47, no. 2, pp. 657–670, Feb. 2001.
[19] *Polar Code Design Rate Matching*, document R1-167209, 3GPP TSG RAN WG1 Meeting #86, Huawei, Gothenburg, Sweden, Aug. 2016.
[20] B. Li, H. Shen, and D. Tse, "An adaptive successive cancellation list decoder for polar codes with cyclic redundancy check," *IEEE Commun. Lett.*, vol. 16, no. 12, pp. 2044–2047, Dec. 2012.

MIN-OH JEONG (S'18) received the B.S. degree in electronic engineering from Inha University, Incheon, South Korea, in 2017, and the M.S. degree in electrical and computer engineering from Ajou University, Suwon, South Korea, in 2019. His main research interests include modern coding theory, wireless communications, and machine learning.

SONG-NAM HONG (S'09–M'14) received the B.Sc. and M.Sc. degrees in electrical and computer engineering from Hanyang University, Seoul, South Korea, in 2003 and 2005, respectively, and the Ph.D. degree in electrical engineering from the University of Southern California (USC), Los Angeles, CA, USA, in 2014. From 2005 to 2009, he was a Research Engineer with the Telecommunication R&D Center, Samsung Electronics, Suwon, South Korea, where he was involved in the standardization of physical layer of the IEEE802.16e/m and LTE systems. From 2014 to 2016, he was a Senior Research Engineer with the Ericsson Research, San Jose, CA, USA, where he has worked for the new communication technologies of 5G and has involved in the standardization of IEEE802.11ay. Since 2016, he has been an Assistant Professor with Ajou University, Suwon. His main research interests include the areas of information theory, coding theory, machine/deep learning, and wireless networks.